species is shown in Fig. 1, where the quantitative similarity in the pattern of repeat sequence expression in the two egg RNA's extends over the full range of transcript sequence concentrations.

The results in Table 1 and Fig. 1 derive from only six cloned repeat sequences and could be nonrepresentative. We attempted to generalize these results by using repetitive DNA tracers prepared from whole sheared *Sp* DNA. As a control, in Fig. 2A the reactions of such a tracer with *Sp* and *Sf* egg RNA's are shown. The kinetics of these reactions are almost indistinguishable, and it follows that the overall distribution of repeat transcript sequence concentrations in the two egg RNA's is similar. The generalization that those repeat families highly represented in *Sp* egg RNA are also highly represented in *Sf* egg RNA is tested in Fig. 2B. A subfraction of the genomic repeat tracer enriched for the sequences prevalent in *Sp* egg RNA was reacted with both egg RNA's. The experiment shows that the repeat sequences prevalent in *Sp* egg RNA are represented in about the same concentrations in *Sf* egg RNA. We conclude that the quantitative similarity in the patterns of repeat sequence representation is general in *Sp* and *Sf* egg RNA's.

The distribution of repeat sequence concentrations in egg RNA is almost certainly physiologically significant. This distribution is highly sequence specific, and different distributions have been found in other RNA's that have been studied. Specific processes of repetitive sequence transcription and RNA accumulation must operate during oogenesis. Our results show that these processes have been adjusted during evolution so as to preserve the repeat transcript sequence concentrations despite significant changes in genomic repeat family sizes and in egg volume and total RNA content. Conceivably all the repeat sequences belonging to expressed families are transcribed in both genomes, but the turnover and transcription rates have altered so as to compensate for the changes in repeat family size. The following argument suggests an alternative view. The particular pattern of repeat sequence representation present in the eggs of both of these species probably existed in their common ancestor as well. Therefore only a subset of the repeats of some repetitive families may be transcribed during oogenesis, since in the cases where the *Sp* families are larger than the *Sf* families this is not reflected in higher *Sp* transcript sequence concentrations. Possibly only repetitive sequence elements of given families which are present in the genomes of both species are expressed. The general implication would be that although multiple homologous repeats are utilized in transcription, these may often represent a subset of the whole genomic sequence family.

Our results emphasize the functional importance of repetitive sequence transcription. The particular pattern of repeat sequence representation in mature eggs is quantitatively conserved between two sea urchin congeners, although the size of the various repeat families in their genomes differs significantly. The repeat sequences themselves have diverged less than single copy sequences during the evolution of this genus (*7*). Conservation of repeat sequence expression suggests that the mechanism restraining change in the primary sequences is evolutionary selection, based on important but unknown functions of the repetitive RNA transcripts.

GORDON P. MOORE
FRANKLIN D. COSTANTINI
JAMES W. POSAKONY
ERIC H. DAVIDSON
Division of Biology, California Institute of Technology, Pasadena 91125
ROY J. BRITTEN
Kerckhoff Marine Laboratory, California Institute of Techology, Corona del Mar 92625

References and Notes

1. F. D. Costantini, R. H. Scheller, R. J. Britten, E. H. Davidson, *Cell* **15**, 173 (1978).
2. R. H. Scheller, F. D. Costantini, M. R. Kozlowski, R. J. Britten, E. H. Davidson, *ibid.*, p. 189.
3. R. H. Scheller *et al.*, *Science* **196**, 197 (1977).
4. This statement is based on the observation that the repeat transcripts of both nuclear and egg RNA's are interspersed with single copy regions in the RNA [M. J. Smith, B. R. Hough, M. E. Chamberlin, E. H. Davidson, *J. Mol. Biol.* **85**, 103 (1974); (*5*)]. However, single copy sequences are always asymmetrically represented in sea urchin RNA's according to studies with both cloned and total DNA tracers [Z. Lev *et al.*, *Dev. Biol.*, in press; B. R. Hough, M. J. Smith, R. J. Britten, E. H. Davidson, *Cell* **5**, 291 (1975); (*5*)]. Therefore, to account for the presence of complementary copies of each repeat sequence, it is necessary to postulate the transcription of multiple repeat elements. The hybrid duplexes formed when cloned repeats are reacted with RNA exhibit heterogeneous thermal stabilities, suggesting that transcription occurs from at least several members of the repeat family (R. H. Scheller, D. M. Anderson, R. J. Britten, E. H. Davidson, unpublished observations).
5. F. D. Costantini, R. J. Britten, E. H. Davidson, in preparation.
6. J. W. Durham, in *Treatise on Invertebrate Paleontology(U) Echinodermata*, R. C. Moore, Ed. (Geological Society of America and Univ. of Kansas Press, New York, 1966), vol. 3, part 1, p. 270.
7. G. P. Moore, R. H. Scheller, E. H. Davidson, R. J. Britten, *Cell* **15**, 649 (1978).
8. Z. Dische and E. Borenfreund, *Biochim. Biophys. Acta* **23**, 639 (1957).
9. A. H. Whiteley, *Am. Nat.* **83**, 249 (1949).
10. The CSp2096 sequence could be a fragment of some highly expressed structural gene or could be related in sequence to such a gene. However, the representation of both complements, and the short length of most of the repeat sequence elements found in egg RNA, argue strongly against the possibility that the repeat transcripts in general code for proteins (*1*). Furthermore, six out of eight repetitive sequence fragments that have been sequenced (*11*) display translation termination signals in all three reading frames of both strands. CSp2096 is exceptional in this regard. In this fragment two reading frames of the strand represented in RNA lack termination codons, though the other strand is translationally blocked in all three frames.
11. J. W. Posakony, R. J. Britten, E. H. Davidson, in preparation.
12. W. H. Klein *et al.*, *Cell* **14**, 889 (1978).
13. B. R. Hough-Evans, B. J. Wold, S. G. Ernst, R. J. Britten, E. H. Davidson, *Dev. Biol.* **60**, 258 (1977).
14. G. P. Moore, W. R. Pearson, E. H. Davidson, R. J. Britten, in preparation.
15. D. M. Anderson *et al.*, in preparation.
16. Supported by NIH grant HD-05753, NIH biomedical research support grant RR-07003, NIH postdoctoral training grant GM-07401, and NIH postdoctoral fellowship GM-07290 (to G.P.M.) and NIH predoctoral training grant GM-07616 (to J.W.P.).

26 December 1979; revised 19 February 1980

Simian Virus 40 Crystals

Abstract. *Small (10 to 150 micrometers) cubic crystals of simian virus 40 have been grown by ammonium sulfate precipitation. Electron micrographs of thin sections from these crystals reveal ordered arrays of virus particles.*

During the past few years a number of crystalline RNA plant viruses have been studied by x-ray diffraction analysis; high-resolution images of tomato bushy stunt virus (*1*) and of southern bean mosaic virus (*2*) have become available. Polyoma became the first animal virus subjected to serious crystallographic investigation (*3, 4*). I now report the crystallization of simian virus 40 (SV40).

In the wild, SV40 causes inapparent infections in certain primates. In the laboratory it can cause tumors in immature animals, and can transform cells in culture. It serves as an important probe in studies of transformation, gene regulation and expression, and DNA replication (*5*). This virus is also of considerable structural interest. It is a nonenveloped particle whose capsid is built on a $T = 7d$ icosahedral surface lattice (*6, 7*). Its 420 subunits are clustered into 12 pentamers and 60 hexamers, giving a total of 72 morphological units or capsomeres in the coat (*7*). The particle diameter has been estimated, from electron microscopy (*8*), as 41 nm and, from x-ray solution scattering (*9*), as 48 nm. The molecular size is 17.6 million daltons (*8*). SV40 is known to code for three coat proteins (VP1, VP2, and VP3). Hexamers contain almost exclusively VP1,

0036-8075/80/0530-1048$00.50/0

and the roles of VP2 and VP3 are not yet clear (*10*).

The SV40 genome is a closed, circular DNA duplex comprising about 5000 base pairs, whose complete nucleotide sequence is known (*11*). The viral DNA is complexed with host cell histones to form a "mini-chromosome" that displays the same nucleosomal organization seen in eukaryotic chromatin. There are about 24 nucleosomes per SV40 particle (*12*). Using model building, Martin (*13*) has shown that a possible mode of packing associates one nucleosome with each of the 20 icosahedral faces of the particle, forming a kind of inner shell, and places the remainder in the center of this shell. Keller and co-workers have obtained electron micrographs of isolated SV40 chromosomes (*12*). These show ordered arrangements of spheres that are identified as nucleosomes. It is difficult to say from inspection whether this arrangement is strictly consistent with Martin's model.

SV40 DNA shows sequence homology with that of polyoma virus, a mouse virus with similar biological characteristics (*14*). Polyoma was first crystallized by Murakami (*3*), but only later were crystals suitable for x-ray diffraction analysis produced (*4*). An x-ray diffraction study of these crystals is now in progress. I have undertaken a parallel study of SV40 because the history of macromolecular crystallography has shown that greater insights emerge when a number of related structures are studied. Further, the crystals of polyoma diffract only to about 0.8 to 0.9 nm resolution. Better crystals would be a great advantage if they could be grown.

Examples of the SV40 crystals produced are shown in Fig. 1. The SV40 (small plaque, strain 776) was grown on BSC-1 cells in tissue culture, initially in a local facility and later at the Massachusetts Institute of Technology, Cell Culture Center. Virus was liberated by freeze-thaw cycles and purified by velocity and equilibrium centrifugation in CsCl. Lipids were removed by extraction with a mixture of chloroform and Triton X-100 detergent. Crystals were grown at 25°C [by the hanging drop technique (*15*)] from a solution containing approximately half-saturated ammonium sulfate buffered with either tris(hydroxymethyl)aminomethane or ammonia to *p*H 7.0 to 7.5, 10 m*M* Mg^{2+} and 0.5 m*M* Ca^{2+}. The concentration of virus was 5 to 10 mg/ml. Morphologically the crystals are cubes, or occasionally tetrahedra, and are nonbirefringent, suggesting a cubic space group. The illustrated crystals are about 10 μm across, but crystals as large as 150 μm have been grown. Virus concentrations in the range 20 to 50 mg/ml are now being used in an effort to produce larger crystals.

Thin sections of these crystals have been examined in the electron microscope, initially to demonstrate that the crystals do indeed contain virus. A num-

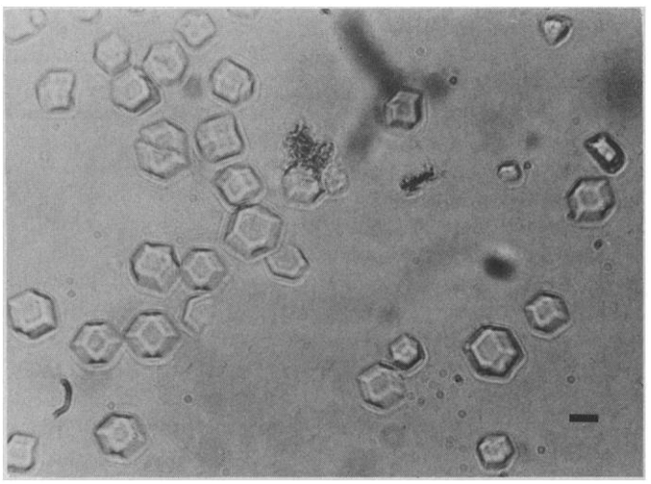

Fig. 1. Light micrograph of small crystals of SV40 showing the cubic morphology. (The scale bar represents 10 μm.)

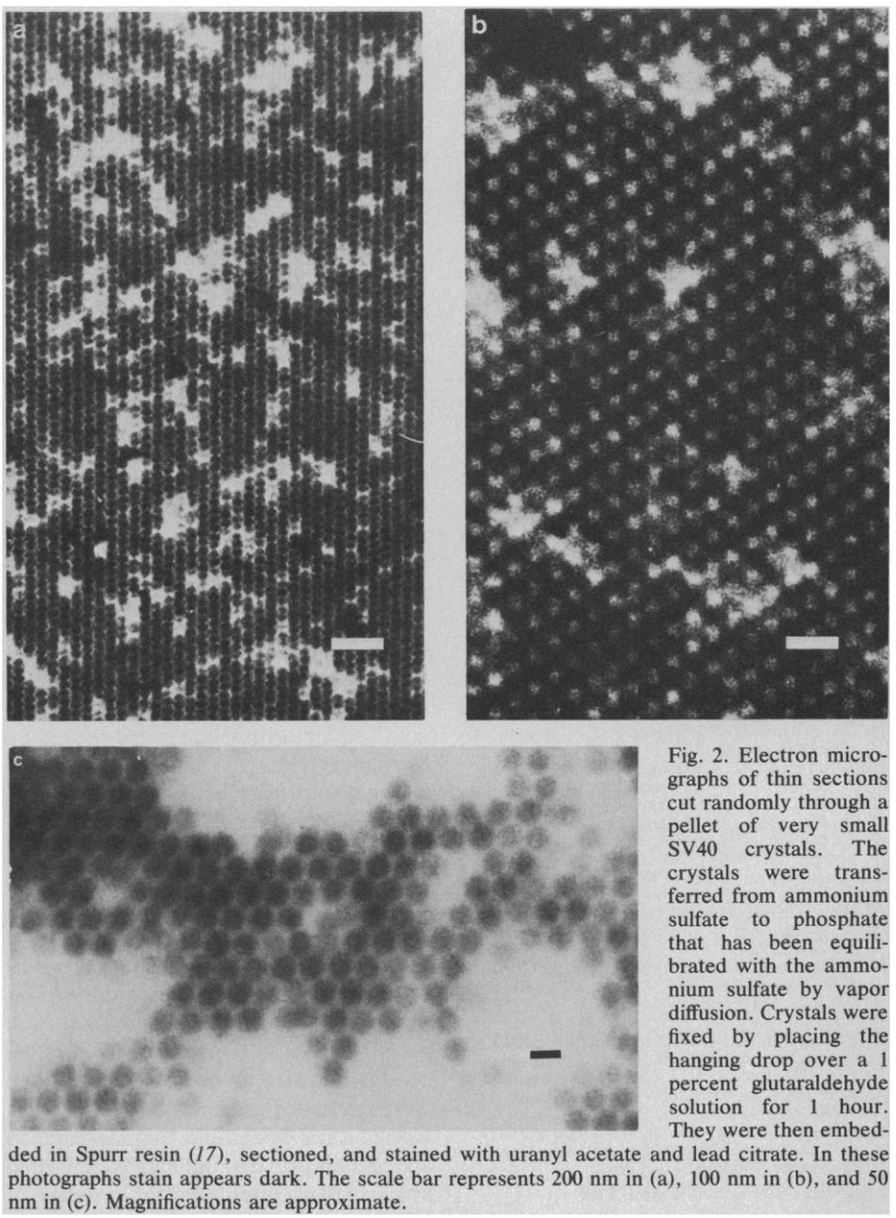

Fig. 2. Electron micrographs of thin sections cut randomly through a pellet of very small SV40 crystals. The crystals were transferred from ammonium sulfate to phosphate that has been equilibrated with the ammonium sulfate by vapor diffusion. Crystals were fixed by placing the hanging drop over a 1 percent glutaraldehyde solution for 1 hour. They were then embedded in Spurr resin (*17*), sectioned, and stained with uranyl acetate and lead citrate. In these photographs stain appears dark. The scale bar represents 200 nm in (a), 100 nm in (b), and 50 nm in (c). Magnifications are approximate.

ber of such sections, cut at random orientations through many small crystals in a pellet, are shown in Fig. 2. Arrays of particles are clearly seen. These micrographs, including others not shown, are strongly suggestive of a cubic lattice. Some, but not all, micrographs show vacancies in the lattice, reminiscent of the vacancies seen in polyoma crystals (*4*). Such vacancies may adversely affect the quality of the diffraction pattern.

The most interesting aspect of SV40 structure is the minichromosome with its constituent nucleosomes. Since the SV40 capsid has icosohedral symmetry, it can be placed in a crystal lattice in 60 equivalent orientations. Since there are not 60 nucleosomes per particle, the nucleosomes themselves cannot have the symmetry of the capsid and must be rotationally disordered in the crystal. Because of this disorder, nucleosomes in the image will appear rotationally averaged, and will therefore be deficient in detail, or perhaps effectively invisible. A low-resolution structure determination, which could be greatly expedited by the use of noncrystallographic symmetry (*16*) would be sufficient to reveal whether any chromatin is likely to be seen.

EATON E. LATTMAN

Department of Biophysics,
Johns Hopkins University
School of Medicine,
Baltimore, Maryland 21205

References and Notes

1. F. K. Winkler, C. E. Schutt, S. C. Harrison, G. Bricogne, *Nature (London)* **265**, 509 (1977).
2. D. Such, I. Rayment, J. E. Johnson, M. G. Rossmann, *Virology* **85**, 187 (1978). M. Rossman informs me that a 2.8-Å structure has been completed.
3. W. T. Murakami, *Science* **142**, 56 (1963).
4. K. W. Adolph, D. L. D. Caspar, C. J. Hollingshead, E. E. Lattman, W. C. Phillips, W. T. Murakami, *ibid.* **203**, 1117 (1979).
5. T. J. Kelly, Jr., and D. Nathans, *Adv. Virus Res.* **21**, 86 (1977).
6. D. L. D. Caspar and A. Klug, *Cold Spring Harbor Symp. Quant. Biol.* **27**, 1 (1962).
7. F. A. Anderer, H. D. Schlumberger, M. A. Koch, H. Frank, H. J. Eggers, *Virology* **32**, 511 (1967).
8. M. A. Koch, H. J. Eggers, F. A. Anderer, H. D. Schlumberger, H. Frank, *ibid.*, p. 503.
9. W. Phillips, D. Schneider, E. E. Lattman, unpublished results.
10. E-S. Huang, M. K. Estes, J. S. Pagano, *J. Virol.* **9**, 923 (1972); G. Christiansen, T. Landers, J. Griffith, P. Berg, *ibid.* **21**, 1079 (1977).
11. W. Fiers *et al. Nature (London)* **273**, 113 (1978).
12. U. Müller, H. Zentgraf, I. Eicken, W. Keller, *Science* **201**, 406 (1978).
13. R. G. Martin, *Virology* **83**, 433 (1977).
14. T. Friedmann, R. F. Doolittle, G. Walter, *Nature (London)* **274**, 291 (1978).
15. A. McPherson, Jr., in *Methods Biochem. Anal.* **23**, 249 (1976).
16. G. Bricogne, *Acta Crystallogr.* **A30**, 395 (1974).
17. C. J. Dawes, *Biological Techniques in Electron Microscopy* (Barnes & Noble, New York, 1971), pp. 71–73.
18. I thank Drs. Daniel Nathans and Thomas J. Kelly, Jr., for advice and for the use of tissue culture facilities; the MIT Cell Culture Center for large-scale virus production; Dr. L. Mario Amzel for help with thin-sectioning. This work supported by NIH grants AI-14820 and AI-00271, and by an internal grant from the Johns Hopkins University School of Medicine.

2 February 1980; revised 2 April 1980

Interaction of Laminae of the Cingulate Cortex with the Anteroventral Thalamus During Behavioral Learning

Abstract. *Neurons in deep laminae of the rabbit cingulate cortex develop discriminative activity at an early stage of behavioral discrimination learning, whereas neurons in the anteroventral nucleus of thalamus and neurons in the superficial cortical laminae develop such activity in a late stage of behavioral learning. It is hypothesized that early-forming discriminative neuronal activity, relayed to anteroventral neurons via the corticothalamic pathway, contributes to the construction of changes underlying the late-forming neuronal discrimination in the anteroventral nucleus. The resultant late discriminative activity in the anteroventral nucleus is then relayed via the thalamocortical pathway back to the superficial cortical laminae, promoting disengagement of cortex from further task-processing.*

A long-standing and intransigent problem in neuroscience has been to identify brain systems mediating learning processes. We now report results of studies of multiple-unit activity recorded from the cingulate area of the cerebral cortex of the rabbit during learning of discriminative avoidance behavior. The results indicate a differential involvement of superficial and deep laminae in mediating acquired discrimination.

The cingulate cortex is reciprocally interconnected with the anteroventral (AV) nucleus of thalamus (*1*). Our results also shed light on the interaction between the cortical laminae and the AV nucleus during learning.

The details of procedure have already been presented (*2*). During avoidance training, we successively presented (in a random order) two tone stimuli, the positive conditional stimulus (CS+) and the negative conditional stimulus (CS−). For each rabbit, the CS+ was either a 1- or an 8-kHz tone (80 dB relative to 0.0002 dyne/cm^2, with a rise time of 3 msec); the CS− was the other tone. The assignment of frequencies to rabbits was counterbalanced. Onset of the CS+ was followed after 5 seconds by constant-current footshock (1.5 mA) delivered to the rabbit through the grid floor of a rotating wheel apparatus (*3*), and terminated by locomotion. Locomotion during the CS+ terminated it and prevented footshock. The CS− was never followed by footshock. Thus, the rabbits learned to avoid footshock by locomoting to the CS+, and they learned not to respond to the CS−. Forty-six rabbits were each given 120 trials daily (60 with each stimulus) until behavioral discrimination reached criterion (*4*). A subset of 29 rabbits received additional sessions of training (overtraining). Before training, each rabbit received a preliminary training session in which tones and the footshock were presented unpaired to provide control data for evaluating training-induced acquisition of discriminative neuronal and behavioral activity (*5*). In order to observe the relationship between neuronal activity and behavioral acquisition, we focused exclusively on neuronal results obtained at certain behaviorally defined stages of acquisition. The stages were preliminary training (PT), the first exposure (FE) to conditioning, the session of first significant (FS) behavioral discrimination (*6*), the session in which the stringent criterion (Cr) of behavioral discrimination was attained, and overtraining. Significant behavioral discrimination did not occur during FE.

Each of the rabbits had a single permanently indwelling metal microelectrode (range of tip lengths, 10 to 60 μm) in cingulate cortex, and 14 of the rabbits had such an electrode in the AV nucleus. Throughout behavioral training, unit activity was fed into high-pass active filters (bandwidth, 500 to 10,000 Hz) and subsequently into pulse-height discriminators set to pass only the three or four largest neuronal spikes. Outputs of the discriminators were fed into a computer programmed to process the neuronal data and to control the behavioral experiment. The computer calculated numerical scores for each session, representing the average frequency of neuronal firing at various periods after CS onset, normalized with respect to the pre-CS baseline. This report concerns the scores representing neuronal activity in the second through the sixth periods of 100 msec. Results of a fine-grained analysis of scores for the first 200 msec will be presented elsewhere (*7*).

Inspection of the brain sections containing the electrode tracks revealed that the recording tips were localized in each of the six laminae that have been distinguished within the cingulate cortex (*8*). An established principle of brain organization states that the superficial laminae (I to IV) of the cerebral cortex are regions which receive axonal input from other brain regions, whereas the deep cortical laminae (V and VI) are regions of origin of axonal outflow to other regions (*9*). Recent anatomical research (*1*)

0036-8075/80/0530-1050$00.50/0